Stereochemical Control of Iron(II) Complexes Containing a Diphosphine Ligand with a Pendant Nitrogen Base

Renee M. Henry,† Richard K. Shoemaker,† Rachel H. Newell,† George M. Jacobsen,† Daniel L. DuBois,*,‡ and M. Rakowski DuBois*,†

Department of Chemistry and Biochemistry, University of Colorado, Boulder, Colorado 80309, and National Renewable Energy Laboratory, 1617 Cole Boulevard, Golden, Colorado 80401

Received February 1, 2005

A series of cis and trans Fe(II) complexes containing the diphosphine ligand PNP (where PNP is bis((diethylphosphino)methyl)methylamine) have been prepared and isolated. These include *cis*-$[Fe(PNP)_2(CH_3CN)_2](BF_4)_2$ (**3**), *cis*-$[Fe(PNP)_2(CH_3CN)(CO)](BF_4)_2$ (**4**), *trans*-$[Fe(PNP)(dmpm)(CH_3CN)_2](BF_4)_2$ (**5**), *trans*-$Fe(PNP)(dmpm)Cl_2$ (**6**), *trans*-$[Fe(PNP)(dmpm)(CO)Cl]_2[FeCl_4]$ (**7**), *trans*-$HFe(PNP)(dmpm)Cl$ (**8**), and *trans*-$[HFe(PNP)(dmpm)(CH_3CN)]BPh_4$ (**9**) (where dmpm is bis(dimethylphosphino)methane). In addition, the cations *trans*-$[HFe(PNP)(dmpm)(CO)]^+$ (**10**) and *trans*-$[(H_2)Fe(PNP)(dmpm)(H)]^+$ (**11**) have been observed in solution. These complexes all possess a pendant base that bridges the two phosphorus atoms of the PNP ligand. A cis geometry is observed for those complexes containing two PNP ligands, whereas a trans geometry is observed for the complexes containing one PNP ligand and one dmpm ligand. The molecular structures of *cis*-$[Fe(PNP)_2(CH_3CN)(CO)](BPh_4)_2$ and *trans*-$[HFe(PNP)(dmpm)(CH_3CN)]BPh_4$ have been confirmed by X-ray diffraction studies. Protonation of **5**, **7**, and **10** occurs at the nitrogen atom of the PNP ligand, and pK_a values are reported for the corresponding protonated complexes. The formation of the dihydrogen complex [*trans*-$[(H_2)Fe(PNP)(dmpm)(H)]^+$ and the protonated PNHP complex *trans*-$[HFe(PNHP)(dmpm)(CO)]^{2+}$ demonstrate that intramolecular heterolytic cleavage of the dihydrogen ligand can be controlled by varying the nature of the ligand trans to the incipient dihydrogen ligand.

Introduction

The ability to oxidize hydrogen to protons using iron complexes is of interest for both practical and fundamental reasons. Iron catalysts for hydrogen oxidation/production would have many advantages for hydrogen fuel cells and electrolyzers for hydrogen production. Iron is cheap, abundant, and not toxic to the environment. In addition, two classes of hydrogenase enzymes, the Fe-only and Ni−Fe hydrogenases, incorporate iron in their active sites. The structures of several hydrogenase enzymes have been determined, and both classes contain bimetallic complexes at the active site.[1−8] Numerous structural models of the active site of the Fe-only hydrogenase enzymes have been reported, and the electrochemical properties and reactions of these compounds with protons and molecular hydrogen have been investigated.[9−18] However, simple bimetallic compounds that catalyze hydrogen oxidation or production with high rates and low overpotentials have proven elusive.

The active site of the Fe-only hydrogenase enzyme from *Desulfovibrio desulfuricans* is depicted by structure **1**. On the basis of recent interpretations of the structural features of the enzyme and its active site, it is thought that a bridging nitrogen atom in the active site assists the heterolytic cleavage of hydrogen and acts as a

* To whom correspondence should be addressed. E-mail: dan_dubois@nrel.gov (D.L.D); mary.rakowski-dubois@colorado.edu (M.R.D.).
† University of Colorado.
‡ National Renewable Energy Laboratory.

(1) Nicolet, Y.; de Lacey, A. L.; Vernède, X.; Fernandez, V. M.; Hatchikian, E. C.; Fontecilla-Camps, J. C. *J. Am. Chem. Soc.* **2001**, *123*, 1596−1601.
(2) Peters, J. W.; Lanzilotta, W. N.; Lemon, B. J.; Seefeldt, L. C. *Science* **1998**, *282*, 1853−1858.
(3) Pereira, A. S.; Tavares, P.; Moura, I.; Moura, J. J. G.; Huynh, B. H. *J. Am. Chem. Soc.* **2001**, *123*, 2771−2782.
(4) Peters, J. W. *Curr. Opinion Struct. Biol.* **1999**, *9*, 670−676.
(5) Volbeda, A.; Garcin, E.; Piras, C.; de Lacey, A. L.; Fernandez, V. M.; Hatchikian, E. C.; Frey, M.; Fontecilla-Camps, J. C. *J. Am. Chem. Soc.* **1996**, *118*, 12989−12996.
(6) Higuchi, Y.; Ogata, H.; Miki, K.; Yasuoka, N.; Yagi, T. *Structure* **1999**, *7,* 549−556.
(7) Garcin, E.; Vernede, X.; Hatchikian, E. C.; Volbeda, A.; Frey, M.; Fontecilla-Camps, J. C. *Structure* **1999**, *7,* 557−565.
(8) Volbeda, A.; Fontecilla-Camps, J. C. *Dalton* **2003**, 4030−4038.
(9) Mejia-Rodriguez, R.; Chong, D.; Reibenspies, J. H.; Soriaga, M. P.; Darensbourg, M. Y. *J. Am. Chem. Soc.* **2004**, *126*, 12004−12014.
(10) Justice, A. K.; Linck, R. C.; Rauchfuss, T. B.; Wilson, S. R. *J. Am. Chem. Soc.* **2004**, *126*, 13214−13215.
(11) Lyon, E. J.; Georgakaki, I. P.; Reibenspies, J. H.; Darensbourg, M. Y. *J. Am. Chem. Soc.* **2001**, *123*, 3268−3278.
(12) Zhao, X.; Georgakaki, I. P.; Miller, M. L.; Yarbrough, J. C.; Darensbourg, M. Y. *J. Am. Chem. Soc.* **2001**, *123*, 9710−9711.
(13) Gloaguen, F.; Lawrence, J. D.; Rauchfuss, T. B. *J. Am. Chem. Soc.* **2001**, *123*, 9476−9477.
(14) Lawrence, J. D.; Li, H.; Rauchfuss, T. B.; Bénard, M.; Rohmer, M.-M. *Angew. Chem., Int. Ed.* **2001**, *40*, 1768−1771.
(15) Evans, D. J.; Pickett, C. J. *Chem. Soc. Rev.* **2003**, *32*, 268−275.
(16) Ott, S.; Kritikos, M.; Åkermark, B.; Sun, L.; Lomoth, R. *Angew. Chem., Int. Ed.* **2004**, *43*, 1006−1009.
(17) Das, P.; Capon, J.-F.; Gloaguen, F.; Pétillon, F. Y.; Schollhammer, P.; Talarmin, J.; Muir, K. W. *Inorg. Chem.* **2004**, *43*, 8203−8205.
(18) Borg, S. J.; Behrsing, T.; Best, S. P.; Razavet, M.; Liu, X.; Pickett, C. J. *J. Am. Chem. Soc.* **2004**, *126*, 16988−16999.

10.1021/om050071c CCC: $30.25
Publication on Web 04/08/2005

shuttle to transfer protons between the active site and the proton conduction channel of the protein.[1,8,14] If this interpretation is correct, then the pendant base plays an important role in the catalytic oxidation/production of hydrogen by iron-only hydrogenases. Studies of metal hydrides with pendant bases suggest that such an interaction is reasonable.[19−22]

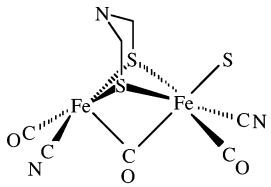

1

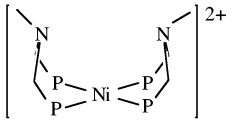

2

Our laboratories have recently reported a simple monometallic nickel complex containing a diphosphine ligand with a pendant nitrogen base, $[Ni(PNP)_2]^{2+}$ (**2**; where PNP is $Et_2PCH_2NMeCH_2PEt_2$).[23] This complex is a catalyst for hydrogen oxidation at low overpotentials. The hydride acceptor ability of the Ni(II) center and the proton acceptor ability of the pendant base are matched in energy to provide a 5 kcal/mol driving force for heterolytic cleavage of hydrogen. In addition, it has been shown that the pendant base provides a pathway for the rapid exchange of the hydride ligand with protons in solution for the catalytic intermediates $[HNi(PNP)_2]^+$ and $[HNi(PNHP)(PNP)_2]^{2+}$ (where PNHP represents the N-protonated form of the PNP ligand).

This paper describes our efforts to synthesize octahedral Fe(II) complexes that incorporate the PNP ligand. Experimental and theoretical studies have shown that the acidity of the coordinated dihydrogen ligand in complexes of the type *trans*-$[(H_2)M(diphosphine)_2(X)]^{n+}$ (where M = Fe, Ru, Os) is strongly dependent on the nature of both X and the diphosphine ligand.[24−27] Strong π acceptors, such as CO ($n = 2$), trans to the dihydrogen ligand result in very acidic complexes, whereas anionic π donors ($n = 1$) result in weakly acidic dihydrogen complexes. Similarly, systematic variation of substituents on the diphosphine ligand cis to the dihydrogen ligand have been reported to result in significant changes in the pK_a values of the dihydrogen ligand. These results suggest that it should be possible to tune the acidity of dihydrogen complexes containing pendant bases to favor either intramolecular heterolytic cleavage of hydrogen or the formation of dihydrogen complexes. In this work it is shown that octahedral Fe(II) complexes containing two PNP ligands adopt cis configurations, whereas Fe(II) complexes containing PNP and dmpm (where dmpm is $Me_2PCH_2PMe_2$) form trans isomers. These results demonstrate that the geometry of these octahedral iron complexes containing a proximal base can be controlled by the proper selection of diphosphine ligands. The different stereochemistries are expected to lead to interesting differences in chemical reactivity as well. The syntheses and reactions of several derivatives of the trans complexes are reported in this paper, and a more complete development of the chemistry of the cis derivatives will be reported in a subsequent paper.

Results

Syntheses and Characterization of Complexes. Addition of $[Fe(CH_3CN)_6](BF_4)_2$ to 2 equiv of the PNP ligand in acetonitrile results in formation of *cis*-$[Fe(PNP)_2(CH_3CN)_2](BF_4)_2$ (**3**), as shown in step 1 of reaction 1. This compound can be isolated as red crystals,

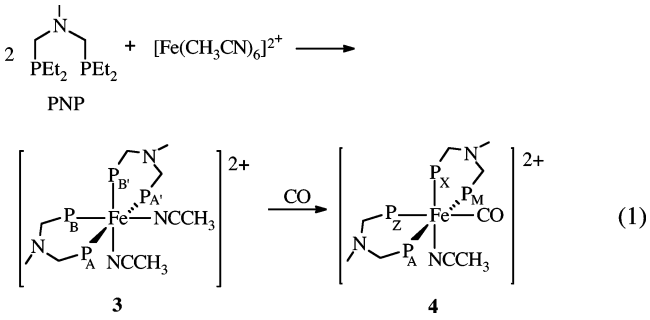

(1)

3 **4**

and it is air-sensitive in solution and in the solid state. The ^{31}P NMR spectrum of this complex in CD_3CN (Figure 1, upward trace) is consistent with an AA′BB′ spin system with resonances centered at 22.0 and 14.5 ppm. This spectrum can be simulated using the parameters listed in the Experimental Section, as shown by the downward trace in Figure 1. The AA′BB′ spin system implies a cis geometry. Resonances for the coordinated PNP ligand are observed in the ^1H NMR spectra recorded in acetonitrile-d_3 (see Experimental Section for specific asignments). ^1H NMR spectra recorded approximately 2 min after adding acetonitrile-d_3 to solid $[Fe(PNP)_2(CH_3CN)_2](BF_4)_2$ showed only free acetonitrile at 1.96 ppm, indicating a half-life of less than 1 min for the exchange of free and coordinated acetonitrile. Similarly, in acetone-d_6, a 10:1 mixture of acetonitrile-d_3 and *cis*-$[Fe(PNP)_2(CH_3CN)_2](BF_4)_2$ results in an 85% loss in the intensity of the bound acetonitrile resonance at 2.73 ppm in 3 min at room temperature (23 ± 2 °C). This corresponds to a $t_{1/2}$ value of approximately 1 min in acetone. Two IR bands (KBr pellets) are observed at 2324 and 2290 cm^{-1}. These bands are assigned to the coordinated acetonitrile ligands. An electrospray ionization mass spectrum (ESI) recorded on acetonitrile solutions resulted in peaks assignable to the parent complex minus a BF_4^- anion and for the sequential loss of the weakly bound acetonitrile ligands. All experimental data are consistent with the formulation of this complex.

Carbon monoxide reacts with *cis*-$[Fe(PNP)_2(CH_3CN)_2](BF_4)_2$ to form *cis*-$[Fe(PNP)_2(CH_3CN)(CO)](BF_4)_2$ (**4**), as shown in step 2 of reaction 1. The four doublet of doublet

(19) Lee, D.-H.; Patel, B. P.; Clot, E.; Eisenstein, O.; Crabtree, R. H. *Chem. Commun.* **1999**, 297−298.
(20) Chu, H. S.; Lau, C. P.; Wong, K. Y.; Wong, W. T. *Organometallics* **1998**, *17*, 2768−2777.
(21) Laugh, A. J.; Park, S.; Ramachandran, R.; Morris, R. H. *J. Am. Chem. Soc.* **1994**, *116*, 8356−8357.
(22) Custelcean, R.; Jackson, J. E. *Chem. Rev.* **2001**, *101*, 1963−1980.
(23) Curtis, C. J.; Miedaner, A.; Ciancanelli, R. F.; Ellis, W. W.; Noll, B. C.; DuBois, M. R.; DuBois, D. L. *Inorg. Chem.* **2003**, *42*, 216−227.
(24) Landau, S. E.; Morris, R. H.; Lough, A. J. *Inorg. Chem.* **1999**, *38*, 6060−6068.
(25) Chin, B.; Lough, A. J.; Morris, R. H.; Schweitzer, C. T.; D'Agostino, C. *Inorg. Chem.* **1994**, *33*, 6278−6288.
(26) Cappellani, E. P.; Drouin, S. D.; Jia, G.; Maltby, P. A.; Morris, R. H.; Schweitzer, C. T. *J. Am. Chem. Soc.* **1994**, *116*, 3375−3388.
(27) Xu, Z.; Bytheway, I.; Jia, G.; Lin, Z. *Organometallics* **1999**, *18*, 1761−1766.

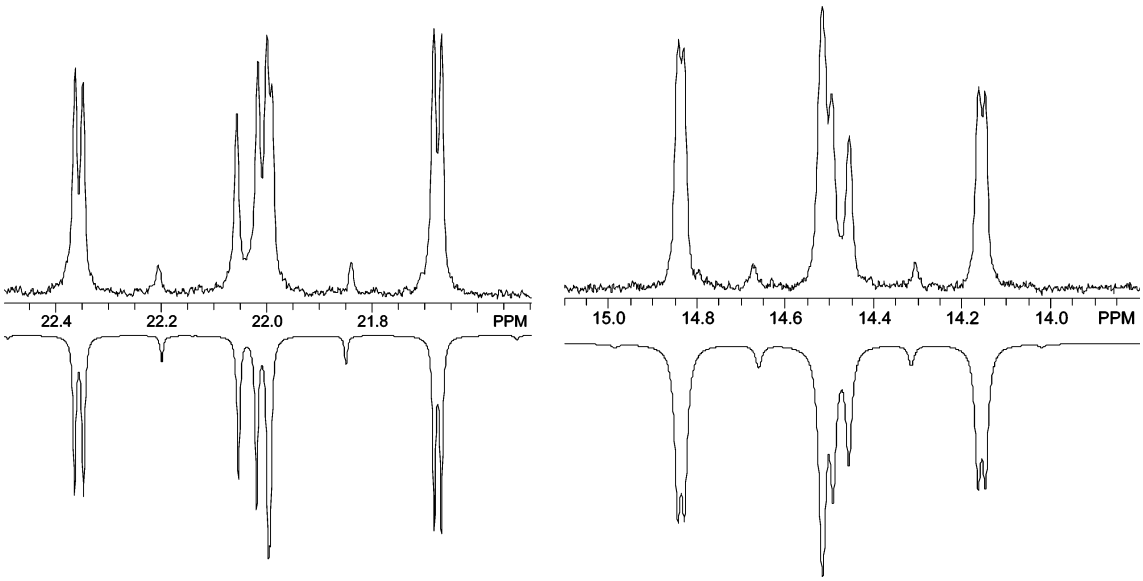

Figure 1. Proton-decoupled ^{31}P NMR spectrum of *cis*-$[Fe(PNP)_2(CH_3CN)_2](BF_4)_2$: (up) experimental spectrum; (down) simulated spectrum. The horizontal scale is in ppm (162 MHz). See the Experimental Section for simulation parameters.

of doublet resonances observed by ^{31}P NMR are consistent with the substitution of just one acetonitrile ligand, resulting in the loss of all symmetry. The simulated spectrum again matches the observed spectrum (see Experimental Section for parameters). In acetonitrile-d_3, the resonance at 2.37 ppm, assigned to coordinated acetonitrile, disappeared with a half-life of 20 min (see Figure S1(a) in the Supporting Information). In acetone-d_6, addition of a 10-fold excess of acetonitrile-d_3 results in the disappearance of the resonance at 2.70 ppm, assigned to coordinated acetonitrile, and the appearance of a resonance at 1.93 ppm, corresponding to free acetonitrile, with a half-life of 34 min. The IR spectrum in solution (CH_2Cl_2) exhibits a band at 1991 cm^{-1} that is assigned to the C−O stretching vibration. The observation of two bands in this region for samples in KBr pellets is attributed to different environments in the solid state. An X-ray diffraction study of *cis*-$[Fe(PNP)_2(CH_3CN)(CO)](BPh_4)_2$, obtained by metathesis of BF_4^- with BPh_4^-, is described below under Structural Studies.

These results indicate that octahedral iron(II) complexes containing two PNP ligands prefer to adopt a cis geometry. In these complexes, unfavorable steric interactions between the ethyl substituents on the two different PNP ligands are expected to disfavor formation of trans complexes. To reduce this interaction, we attempted to prepare *trans*-$[Fe(PNP)(dppm)(CH_3CN)_2](BF_4)_2$ (where dppm is bis(diphenylphosphino)methane) by reacting $[Fe(CH_3CN)_6](BF_4)_2$, PNP, and dppm in a 1:1:1 ratio. It was encouraging that some of the desired product appeared to form, as indicated by ^{31}P NMR spectroscopy of the crude reaction mixture (see Experimental Section), but the reaction was not sufficiently clean to be an attractive synthetic approach. However, reaction of $[Fe(CH_3CN)_6](BF_4)_2$, PNP, and dmpm (where dmpm is bis(dimethylphosphino)methane) in a 1:1:1 ratio, as shown in reaction 2, resulted in the formation of *trans*-$[Fe(PNP)(dmpm)(CH_3CN)_2](BF_4)_2$ (**5**), in 55% isolated yield. The ^{31}P NMR spectrum of this red complex is shown in the upward trace of Figure 2, and the simulated spectrum is shown by the downward trace. The four phosphorus nuclei form an AA′XX′ spin system, which is consistent with a trans geometry, but not with a cis geometry, which would result in four nonequivalent nuclei. A singlet at 2.40 ppm in the ^1H NMR spectrum recorded in CD_3CN is assigned to coordinated acetonitrile. This resonance disappears with a half-life of approximately 7.2 h at 23 ± 2 °C. This observation indicates that the acetonitrile ligands in this complex are not as labile as those of *cis*-$[Fe(PNP)_2(CH_3CN)_2](BF_4)_2$ described above ($t_{1/2}$ < 1 min). The IR spectrum, mass spectrum, and elemental analyses of this complex (see Experimental Section) are also consistent with the formulation of **5**.

$$[Fe(CH_3CN)_6](BF_4)_2 + PNP + dmpm \longrightarrow \left[\text{Fe(PNP)(CH}_3\text{CN)}_2\right](BF_4)_2 \quad (2)$$

5

Several additional trans derivatives have been synthesized and isolated, as detailed in the Experimental Section. Reaction of $FeCl_2$ with a 1:1 mixture of PNP and dmpm results in the formation of the emerald green (λ_{max} 673 nm, ϵ = 17 M^{-1} cm^{-1}) paramagnetic complex *trans*-Fe(PNP)(dmpm)Cl_2 (**6**; step 1 of reaction 3). This

$$FeCl_2 + PNP + dmpm \rightarrow \underset{\mathbf{6}}{\textit{trans}\text{-Fe(PNP)(dmpm)Cl}_2} \xrightarrow{CO} \underset{\mathbf{7}}{\textit{trans}\text{-[Fe(PNP)(dmpm)(CO)Cl]}^+} \quad (3)$$

complex is similar to the previously reported Fe(diphosphine)$_2$$Cl_2$ complexes containing the ligands 1,2-bis(diphenylphosphino)ethane (dppe) and 1,2-bis(diethylphosphino)ethane (depe).[28−30] Generation of this complex in situ followed by reaction with CO (1 atm) results in the formation of *trans*-[Fe(PNP)(dmpm)(CO)-

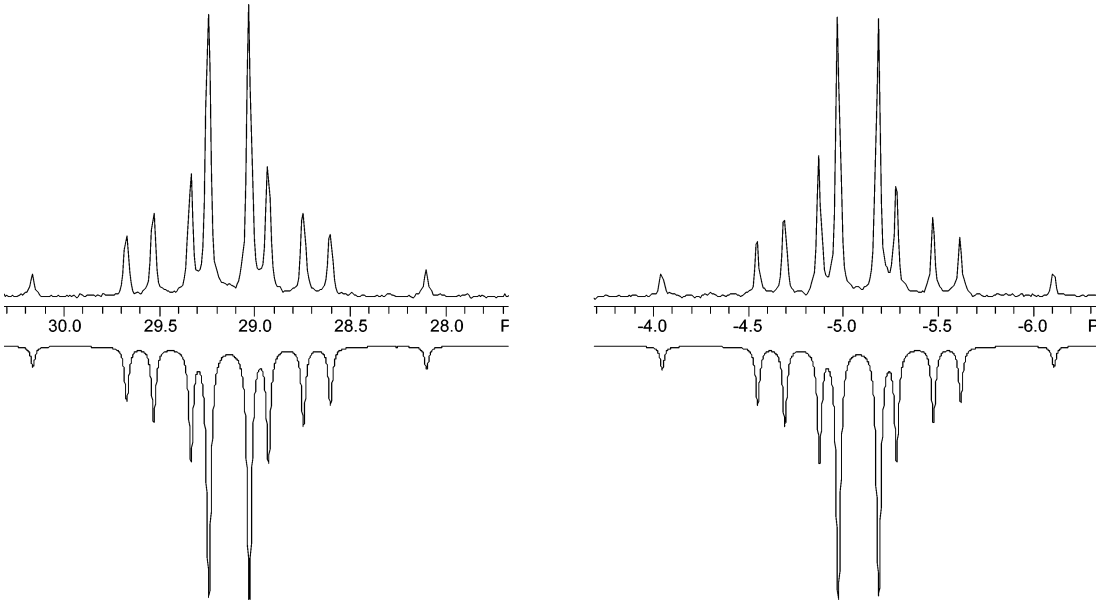

Figure 2. Proton-decoupled ^{31}P NMR spectrum of *trans*-[Fe(PNP)(dmpm)$(CH_3CN)_2$]$(BF_4)_2$: (up) experimental spectrum; (down) simulated spectrum. The horizontal scale is in ppm (162 MHz).

$Cl]_2[FeCl_4]$ (**7;** step 2 of reaction 3).[31] The ^{31}P NMR spectrum of this carbonyl complex is again consistent with a trans geometry. The observation by IR spectroscopy of a single CO stretching frequency at 1936 cm^{-1} in dichloromethane solution suggests the presence of one carbonyl ligand, which is also consistent with the observation of the $[Fe(PNP)(dmpm)(CO)Cl]^+$ cation (*m/z* 490) by ESI mass spectrometry.

Reaction of $Fe(PNP)(dmpm)Cl_2$ with bis(triphenylphosphine)iminium borohydride in tetrahydrofuran (THF) produces orange *trans*-HFe(PNP)(dmpm)Cl (**8**), which is isolated in low to moderate yields. The ^{31}P NMR spectrum indicates an AA′XX′ spin system and a trans geometry. The presence of a hydride ligand is confirmed by the observation of a pentet resonance with $^2J_{PH}$ = 47 Hz at −27.0 ppm in the ^1H NMR spectrum and an IR band at 1797 cm^{-1} assigned to the Fe−H stretching mode. In comparison, the complex $HFe(depe)_2Cl$ has a hydride resonance at −29.1 ppm and an IR stretch at 1849 cm^{-1}.[29,30] An ESI mass spectrum of an acetonitrile solution of **8** exhibited fragments consistent with loss of chloride, loss of hydride, and the formation of $[HFe(PNP)(dmpm)(CH_3CN)]^+$. The latter cation presumably forms by loss of chloride and solvent coordination, as discussed in the next paragraph. Elemental analysis of **8** indicates the presence of only one chloride ligand, and UV−visible data indicate that contamination with *trans*-$Fe(PNP)(dmpm)Cl_2$ is less than 5%.

As shown on the left side of Scheme 1, reaction of *trans*-HFe(PNP)(dmpm)Cl with acetonitrile in the presence of sodium tetraphenylborate results in the formation of *trans*-$[HFe(PNP)(dmpm)(CH_3CN)](BPh_4)$ (**9**). The ^{31}P NMR spectrum again indicates an AA′XX′ spin system and a trans geometry. The presence of a hydride

Scheme 1

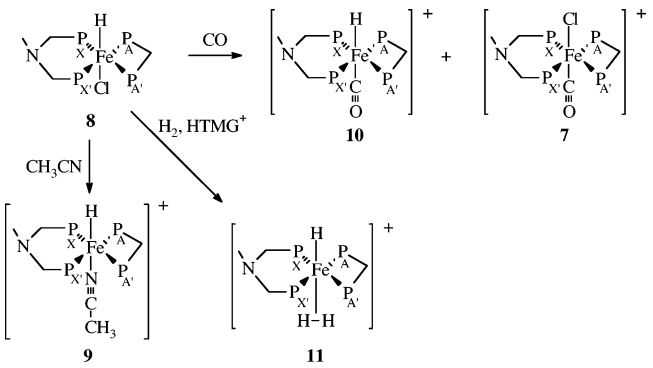

ligand is confirmed by the observation of a triplet of triplet of doublets at −19.8 ppm in the ^1H NMR spectrum. The triplet patterns arise from coupling to the two pairs of phosphorus atoms associated with the PNP and dmpm ligands, as indicated by broadband and selective phosphorus decoupling experiments described in the Experimental Section. The origin of the doublet splitting of the hydride resonance is attributed to coupling between the hydride ligand and one of the protons of the methylene group of the dmpm ligand. A broadband ^{31}P-decoupled ^1H NMR spectrum exhibits an AB portion of an ABX spin system at 2.98 and 3.15 ppm ($^2J_{HH}$ = 14 Hz) assigned to the methylene protons of the dppm ligand. The resonance at 3.15 ppm exhibits an additional coupling of 4 Hz. This coupling matches that of the doublet splitting observed for the hydride resonance. A broadband ^{31}P-decoupled ^1H gCOSY spectrum (Figure S2 in the Supporting Information) confirmed the coupling between the resonance at 3.15 ppm and the hydride resonance at −19.8 ppm. An IR band at 1826 cm^{-1} is assigned to the Fe−H stretching mode. As expected, the frequency of this band is about 30 cm^{-1} higher than that of *trans*-HFe(PNP)(dmpm)Cl. The coordinated acetonitrile ligand in this complex exchanges slowly with free acetonitrile. A singlet at 2.22 ppm in the ^1H NMR spectrum is assigned to the coordinated acetonitrile in CD_3CN. This resonance

(28) Chatt, J.; Hayter, R. G. *J. Chem. Soc.* **1961**, 5507−5511.
(29) Aresta, M.; Giannoccaro, P.; Rossi, M.; Sacco, A. *Inorg. Chim. Acta* **1971**, *5*, 115−118.
(30) Mayes, M. J.; Prayter, B. E. *Inorg. Synth.* **1974**, *15*, 22−25.
(31) A similar compound, $[FeCl(CO)(dppe)_2][FeCl_4]$, has been previously reported: Gao, Y.; Holah, D. G.; Hughes, A. N.; Spivak, G. J.; Havighurst, M. D.; Magnuson, V. R.; Polyakov, V. *Polyhedron* **1997**, *16*, 2797−2807.

slowly disappears with a half-life of 9.6 h at 23 ± 2 °C (Figure S1(b)). An X-ray diffraction study of *trans*-[HFe(PNP)(dmpm)(CH_3CN)](BPh_4) is described below under Structural Studies.

Reaction of *trans*-[HFe(PNP)(dmpm)Cl] with CO and $NaPF_6$ in acetone-d_6 in an NMR tube (top reaction in Scheme 1) results in a 60/40 mixture of *trans*-[HFe(PNP)(dmpm)(CO)]$^+$ (**10**) and *trans*-[Fe(PNP)(dmpm)(Cl)(CO)]$^+$. The latter is spectroscopically identical with the material obtained from the reaction of CO with Fe(PNP)(dmpm)Cl_2 discussed above. The expected product, *trans*-[HFe(PNP)(dmpm)(CO)]$^+$, has a hydride resonance at −7.06 ppm in the ^{1}H NMR spectrum that appears as a triplet of triplet of doublets. As discussed for the analogous acetonitrile complex, this coupling pattern can be attributed to coupling to the two diphosphine ligands and a proton of the methylene group of the dmpm ligand. The ^{31}P NMR spectrum exhibits an AA′XX′ spectrum centered at 2.34 ppm (dmpm) and 44.29 ppm (PNP), as expected for a trans geometry. Attempts to isolate *trans*-[HFe(PNP)(dmpm)(CO)]$^+$ as a pure compound were unsuccessful. The origin of *trans*-[Fe(PNP)(dmpm)(Cl)(CO)]$^+$, produced as a significant side product in this reaction, is not known. The UV−visible spectra of the starting materials indicate that less than 5% of the original material is Fe(PNP)(dmpm)Cl_2, which would be expected to give rise to *trans*-[Fe(PNP)(dmpm)(Cl)(CO)]$^+$ when treated with CO. The observation that *trans*-[HFe(PNP)(dmpm)Cl reacts with CO in acetone-d_6 to form a 60/40 mixture of *trans*-[HFe(PNP)(dmpm)(CO)]$^+$ and *trans*-[Fe(PNP)(dmpm)(Cl)(CO)]$^+$ indicates that the major portion of the *trans*-[Fe(PNP)(dmpm)(Cl)(CO)]$^+$ complex is produced by a hydride transfer reaction, but we have been unable to identify the hydride acceptor. However, this reaction is very reproducible.

When *trans*-[HFe(PNP)(dmpm)Cl] is reacted with H_2 in the presence of 1 equiv of the tetramethylguanidinium cation ($HTMG^+$) in acetone-d_6 at 0 °C in an NMR tube for 1.5 h (diagonal reaction in Scheme 1), broad resonances are observed in the ^{1}H NMR spectrum at −7.9 and −11.4 ppm that are assigned to the species [(H_2)Fe(PNP)(dmpm)H]$^+$ (**11**). Upon cooling to −60 °C, these resonances sharpen into a pentet centered at −11.76 ppm ($^2J_{PH}$ = 46 Hz) and a singlet at −7.90 ppm with an integration ratio of 1.0:2.0. The former is assigned to the hydride ligand and the latter to the dihydrogen ligand of [(H_2)Fe(PNP)(dmpm)H]$^+$. When the sample is warmed back up to 0 °C, the original spectrum is observed. The exchange of a hydride ligand with an H_2 ligand has been observed for a number of other [(H_2)Fe(diphosphine)$_2$H]$^+$ complexes.[32−35] Temperature-dependent T_1 measurements of these resonances at 400 MHz gives a T_1 value of 346 ms at −90 °C for the hydride ligand and a value of 20.7 ms at −90 °C for the resonance assigned to the dihydrogen ligand. A plot of ln T_1 versus 1/K is shown in Figure S3 in the Supporting Information. Using the T_1 value obtained at −90 °C for T_1^{min}, a H−H distance of 0.89 Å can be calculated, assuming rapid rotation of the dihydrogen ligand, and a H−H distance of 1.12 Å, assuming slow rotation.[36−38] Dihydrogen complexes of iron with a trans hydride ligand generally exhibit rapid rotation.[39] However, the T_1 value obtained for the dihydrogen ligand at the lowest temperature of −90 °C may not be a true minimum. To obtain a $^1J_{HD}$ value for calculating the H−H bond distance, the reaction of *trans*-[HFe(PNP)(dmpm)Cl] with deuterated tetramethylguanidinium under HD gas in protioacetone was followed by ^{2}H NMR. A doublet ($^1J_{HD}$ = 30.8 Hz) observed at −8.01 ppm for a spectrum recorded at −60 °C is assigned to the HD ligand. Upon proton decoupling, this resonance collapses to a singlet. A H−H bond distance of 0.90−0.92 Å was calculated using this $^1J_{HD}$ value and relationships proposed by Heinekey and Morris.[40,41] The data above are consistent with the formation of the dihydrogen complex [(H_2)Fe(PNP)(dmpm)H]$^+$ with an H−H bond distance similar to that observed for [(H_2)Fe(dppe)$_2$H]$^+$ (0.92−0.94 Å from $^1J_{HD}$).[33,34] The *trans*-[(H_2)Fe(PNP)(dmpm)H]$^+$ complex is always accompanied by a significant fraction of the starting complex, *trans*-[HFe(PNP)(dmpm)Cl], or a decomposition product tentatively identified as the *cis*-dihydride, [$(H)_2$Fe(PNP)(dmpm)]. As a result, the dihydrogen complex was not isolated.

Protonation of Complexes Containing the PNP Ligand. Protonation reactions of *trans*-[Fe(PNP)(dmpm)(CH_3CN)$_2$]$^{2+}$, *trans*-[Fe(PNP)(dmpm)(Cl)(CO)]$^+$, and *trans*-[HFe(PNP)(dmpm)(CO)]$^+$ were studied in acetonitrile at 23 ± 2 °C (reaction 4). The use of strong acids

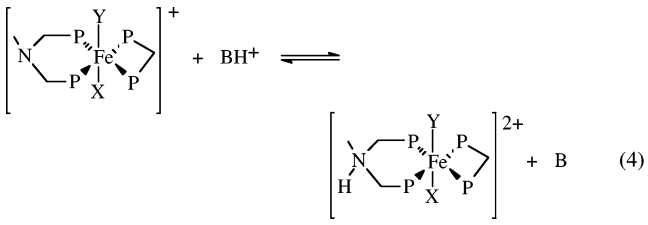

(4)

X	Y	B	K_{eq}	pK_a
CH_3CN	CH_3CN	*p*-$BrC_6H_4NH_2$	0.6 ± 0.2	9.4 ± 0.2
CO	Cl	*p*-$BrC_6H_4NH_2$	1.1 ± 0.2	9.6 ± 0.2
CO	H	$C_6H_5NH_2$	0.9 ± 0.2	10.5 ± 0.2

such as HBF_4 and cyanoanilinium (pK_a = 7.5 in acetonitrile)[42] resulted in complete protonation of the PNP ligand, as indicated by a constant shift in the resonance assigned to the PNHP$^+$ ligand when excess acid was used. The use of weaker acids such as anisidinum (pK_a = 11.3), anilinium (pK_a = 10.6), and bromoanilinium (pK_a = 9.6)[42] resulted in smaller shifts intermediate

(32) Hills, A.; Hughes, D. L.; Jimenez-Tenorio, M.; Leigh, G. J. *J. Chem. Soc., Dalton Trans.* **1993**, 3041−3049.
(33) Morris, R. H.; Sawyer, J. F.; Shiralian, M.; Zubkowski, J. D. *J. Am. Chem. Soc.* **1985**, *107*, 5581−5582.
(34) Ricci, J. S.; Koetzle, T. F.; Bautista, M. T.; Hofstede, T. M.; Morris, R. H.; Sawyer, J. F. *J. Am. Chem. Soc.* **1989**, *111*, 8823−8827.
(35) Gilbertson, J. D.; Szymczak, N. K.; Tyler, D. R. *Inorg. Chem.* **2004**, *43*, 3341−3343.
(36) Kubas, G. J. In *Metal Dihydrogen and σ-Bond Complexes*; Fackler, J. P., Jr., Ed.; Modern Inorganic Chemistry; Kluwer Academic/Plenum: New York, 2001; p 159.
(37) Morris, R. H. *Can. J. Chem.* **1996**, *74*, 1907−1915.
(38) Morris, R. H.; Wittebort, R. J. *Magn. Reson. Chem.* **1997**, *35*, 243.
(39) Gusev, D. G.; Kuhlman, R. L.; Renkema, K. B.; Eisenstein, O.; Caulton, K. G. *Inorg. Chem.* **1996**, *35*, 6775−6783.
(40) Luther, T. A.; Heinekey, M. *Inorg. Chem.* **1998**, *37*, 127−132.
(41) Maltby, P. A.; Schlaf, M.; Steinbeck, M.; Lough, A. J.; Morris, R. H.; Klooster, W. T.; Koetzle, T. F.; Srivastava, R. C. *J. Am. Chem. Soc.* **1996**, *118*, 5396−5407.
(42) Edidin, R. T.; Sullivan, J. M.; Norton, J. R. *J. Am. Chem. Soc.* **1987**, *109,* 3945−3953.

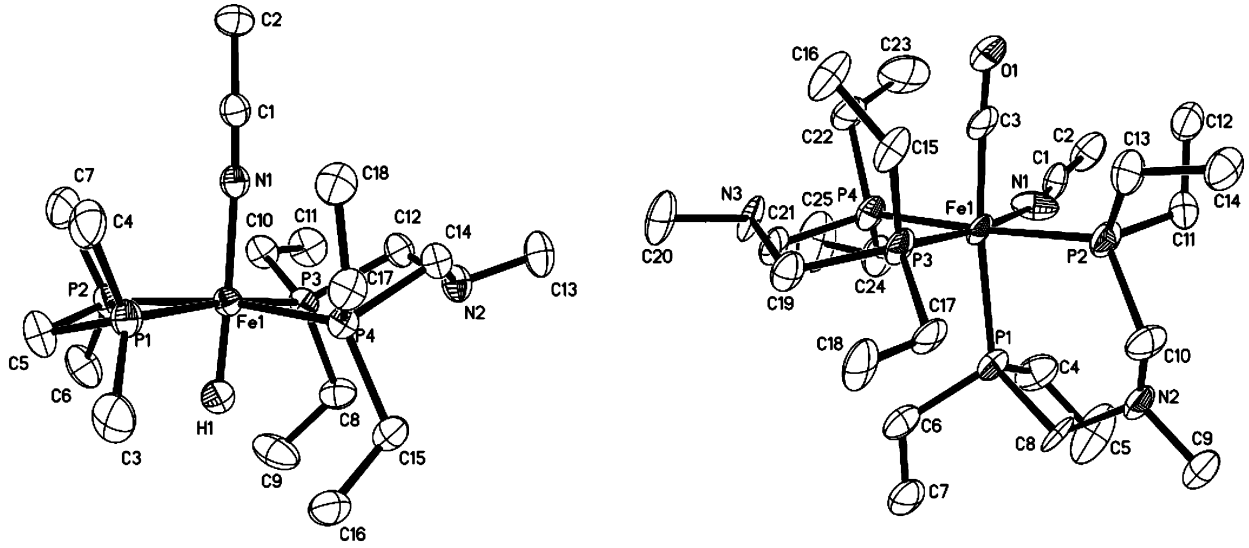

Figure 3. Drawings of the *trans*-[HFe(PNP)(dmpm)(CH_3CN)]$^+$ (left) and *cis*-[Fe(PNP)$_2$(CH_3CN)(CO)]$^{2+}$ (right) cations, indicating the atom-numbering schemes. Thermal ellipsoids are drawn at the 50% probability level.

between those of the fully protonated species and the unprotonated species. These shifts could be used to determine the equilibrium constants shown below reaction 4 (see Experimental Section for details).[43] These equilibrium constants were used to calculate the pK_a values of the coordinated PNHP$^+$ ligands in acetonitrile by adding log K_{eq} to the pK_a value of the corresponding protonated base. The pK_a values of *trans*-[Fe(PNHP)(dmpm)(CH_3CN)$_2$]$^{3+}$ (9.4), *trans*-[Fe(PNHP)(dmpm)(Cl)(CO)]$^{2+}$ (9.6), and *trans*-[HFe(PNHP)(dmpm)(CO)]$^{2+}$ (10.5) in acetonitrile are similar to previously determined values for [HNi(PNHP)(PNP)]$^{2+}$ (10.6), [Ni(PNHP)(dmpm)]$^{3+}$ (8.7), and [Fe$_2${(SCH$_2$)$_2$N(H)Me}(CO)$_6$]$^+$ (7.6−10.6).[14,23] The uncertainties indicated for the equilibrium constants of the iron complexes are for 2 standard deviations based on 3−5 independent measurements. The uncertainties in the pK_a values include the uncertainties in these equilibrium measurements, as well as the uncertainty in the pK_a values of the protonated bases that are used as references (±0.1).

In the case of *trans*-[HFe(PNP)(dmpm)(CH_3CN)]$^+$, protonation of the PNP ligand is followed by a slow loss of H_2 and the formation of *trans*-[Fe(PNP)(dmpm)(CH_3CN)$_2$]$^{2+}$. The observed hydrogen loss from *trans*-[HFe(PNHP)(dmpm)(CH_3CN)]$^{2+}$ when anisidine is used as a base under 1 atm of H_2 can be used to calculate a hydride donor ability of less than 61 kcal/mol for [HFe(PNP)(dmpm)(CH_3CN)]$^+$ (see the Supporting Information for details).[44] The hydride donor ability is the free energy associated with the reaction of [HFe(PNP)(dmpm)(CH_3CN)]$^+$ to form [Fe(PNP)(dmpm)(CH_3CN)$_2$]$^{2+}$ and H$^-$ in acetonitrile. Because coordination of acetonitrile occurs in the course of this reaction, the solvent plays an important role in determining the energetics of this hydride transfer reaction. The hydride donor ability of less than 61 kcal/mol for [HFe(PNP)(dmpm)(CH_3CN)]$^+$ compared to a value of 67 kcal/mol for [HNi(PNP)$_2$]$^+$ (also measured in acetonitrile) indicates that the iron complex is at least a 6 kcal/mol better hydride donor than the nickel complex.[23]

Table 1. Selected Bond Distances (Å) and Bond Angles (deg)

trans-[HFe(PNP)(dmpm)(CH_3CN)]$^+$		*cis*-[Fe(PNP)$_2$(CH_3CN)(CO)]$^{2+}$	
Bond Distances			
Fe(1)−N(1)	1.9186(18)	Fe(1)−C(3)	1.795(7)
Fe(1)−P(4)	2.2044(6)	Fe(1)−N(1)	1.990(5)
Fe(1)−P(2)	2.2159(6)	Fe(1)−P(3)	2.297(2)
Fe(1)−P(3)	2.2173(6)	Fe(1)−P(2)	2.302(2)
Fe(1)−P(1)	2.2217(6)	Fe(1)−P(4)	2.321(2)
Fe(1)−H(1)	1.53(2)	Fe(1)−P(1)	2.379(2)
N(1)−C(1)	1.151(3)	N(1)−C(1)	1.118(8)
		C(3)−O(1)	1.142(7)
Bond Angles			
N(1)−Fe(1)−P(4)	94.68(5)	C(3)−Fe(1)−P(3)	87.7(2)
N(1)−Fe(1)−P(2)	93.78(5)	N(1)−Fe(1)−P(2)	88.7(2)
P(4)−Fe(1)−P(2)	168.28(2)	C(3)−Fe(1)−P(2)	87.1(2)
N(1)−Fe(1)−P(3)	89.63(5)	N(1)−Fe(1)−P(3)	173.4(2)
P(4)−Fe(1)−P(3)	89.58(2)	P(3)−Fe(1)−P(4)	90.89(7)
P(2)−Fe(1)−P(3)	98.58(2)	P(3)−Fe(1)−P(2)	95.42(7)
N(1)−Fe(1)−P(1)	97.75(6)	N(1)−Fe(1)−P(1)	87.93(17)
P(4)−Fe(1)−P(1)	97.18(2)	P(4)−Fe(1)−P(1)	94.02(7)
P(2)−Fe(1)−P(1)	73.63(2)	P(2)−Fe(1)−P(1)	87.62(7)
P(3)−Fe(1)−P(1)	169.52(2)	P(3)−Fe(1)−P(1)	97.36(8)
H(1)−Fe(1)−P(1)	81.1(10)	C(3)−Fe(1)−P(1)	173.0(2)
H(1)−Fe(1)−P(2)	83.9(9)	C(3)−Fe(1)−P(4)	90.7(2)
H(1)−Fe(1)−P(3)	91.2(10)	N(1)−Fe(1)−P(4)	84.8(2)
H(1)−Fe(1)−P(4)	87.5(9)	P(2)−Fe(1)−P(4)	173.22(7)
H(1)−Fe(1)−N(1)	177.7(10)	C(3)−Fe(1)−N(1)	87.4(3)
Fe(1)−N(1)−C(1)	174.49(17)	C(1)−N(1)−Fe(1)	166.5(7)
		N(1)−C(1)−C(2)	174.8(8)

Structural Studies. A structural determination of *trans*-[HFe(PNP)(dmpm)(CH_3CN)](BPh_4) was carried out on crystals grown from an acetonitrile/ether solution. A drawing of the cation is shown on the left side of Figure 3, and selected bond angles and bond distances are given in Table 1. The hydride ligand and the acetonitrile ligand occupy trans positions. The six-membered ring formed by iron and the PNP ligand is in the chair conformation, as observed in previous nickel structures.[23] The four-membered ring formed by iron and dmpm is folded toward the hydride ligand with a distance of 3.13 Å between the hydride ligand and the nearest hydrogen atom of the methylene bridge of the

(43) Drago, R. S. *Physical Methods for Chemists,* 2nd ed.; Surfside Scientific: Gainesville, FL, 1992; pp 290−295.

(44) Curtis, C. J.; Miedaner, A.; Ellis, W. W.; DuBois, D. L. *J. Am. Chem. Soc.* **2002**, *124*, 1918−1925.

dmpm ligand. The Fe−P, Fe−N, and Fe−H distances are all within ranges observed for similar low-spin Fe(II) complexes.[32−34] The phosphorus atoms of both diphosphine ligands are slightly bent toward the hydride ligand and away from acetonitrile with an average N(1)−Fe(1)−P angle of 94.0°. The average N(1)−Fe(1)−P bond angle is slightly larger for the dmpm ligand (95.8°) than for the PNP ligand (92.2°). This may be a reflection of the small dihedral angles between the methyl groups of the dmpm ligand and the coordinated acetonitrile ligand (i.e., N(1)−Fe(1)−P(2)−C(7) = 2.3° and N(1)−Fe(1)-P(1)−C(4) = 10.2°). The P(1)−Fe(1)−P(2) bond angle for the dmpm ligand (73.6°) is much less than 90°, as expected, and the P(3)−Fe(1)−P(4) angle of the PNP ligand (89.6°) is very close to the ideal 90°. These observed bond angles are similar to those observed for $[Ni(PNP)(dmpm)]^{2+}$: 73.8 and 94.2°, respectively.[20]

An X-ray diffraction study of *cis*-$[Fe(PNP)_2(CH_3CN)(CO)](BPh_4)_2$ confirms the geometry assigned on the basis of spectrosopic data for cation **4**. A drawing of this cation is shown on the right side of Figure 3, and selected bond distances and angles are given in Table 1. The acetonitrile and carbonyl ligands occupy cis positions with a N(1)−Fe(1)−C(3) angle of 87.4°. The three angles defined by cis diethylphosphino groups not constrained to a chelate ring, i.e., P(1)−Fe(1)−P(3), P(1)−Fe(1)−P(4), and P(2)−Fe(1)−P(3), average 95.6°. The two bond angles between phosphorus atoms within a chelate ring, P(1)−Fe(1)−P(2) and P(3)−Fe(1)−P(4), average 89.2°. Taken together, these bond angles suggest that steric interactions between cis diethylphosphino groups not constrained to a chelate ring produce a distortion of these groups toward the smaller CO and acetonitrile ligands. In addition, the N(1)−Fe(1)−P(2)−C(11) torsional angle is 5.5°, indicating that the acetonitrile ligand and an ethyl group on P(2) are essentially eclipsed. As a result, the P(2)−Fe(1)−N(1) angle (88.7°) is slightly larger than the P(4)−Fe(1)−N(1) angle (84.8°), and the acetonitrile ligand bends away from the ethyl group on P(2) toward P(4); i.e., the Fe(1)−N(1)−C(1) angle is 166.5°. A similar interaction occurs between acetonitrile and C(4) (N(1)−Fe(1)−P(1)−C(4) = 3.9°). A somewhat less eclipsed form is observed for the CO ligand and the axial substituents on P(3) and P(4) (C(3)−Fe(1)−P(4)−C(22) = 12.0° and C(3)−Fe(1)−P(3)−C(15) = 12.4°). The average Fe−P bond distance for cation **4** is 2.32 Å. This distance is 0.11 Å longer than the average Fe−P distance observed for the *trans*-$[HFe(PNP)(dmpm)(CH_3CN)]^+$ cation discussed in the preceding paragraph. The Fe(1)−P(1) distance in **4** is at least 0.06 Å longer than the three remaining Fe−P bond lengths, because of the greater trans influence of the CO ligand. The Fe(1)−N(1) distance of 1.99 Å for $[Fe(PNP)_2(CH_3CN)(CO)]^{2+}$ is also significantly longer than the Fe(1)−N(1) distance of 1.92 Å for *trans*-$[HFe(PNP)(dmpm)(CH_3CN)]^+$. This larger bond distance is consistent with the greater lability of the acetonitrile ligand of *cis*-$[Fe(PNP)_2(CH_3CN)(CO)]^{2+}$ compared to *trans*-$[HFe(PNP)(dmpm)(CH_3CN)]^+$.

Discussion

In general, octahedral complexes containing two diphosphine ligands with large chelate bites form cis complexes.[25,45,46] Therefore, the formation of *cis*-$[Fe(PNP)_2(CH_3CN)_2](BF_4)_2$ from $[Fe(CH_3CN)_6](BF_4)_2$ and 2 equiv of PNP, as shown in step 1 of reaction 1, is expected. The substitution of one ligand, as shown in step 2, to form *cis*-$[Fe(PNP)_2(CH_3CN)(CO)](BF_4)_2$ indicates that stepwise substitution of acetonitrile in this complex may be a useful route to forming a series of cis complexes containing a diphosphine ligand with a pendant base. Further studies toward this end are in progress in our laboratories. The cis geometry of $[Fe(PNP)_2(CH_3CN)(CO)](BPh_4)_2$ has been confirmed by an X-ray diffraction study.

A more extensively studied class of dihydrogen complexes are the *trans*-$[(H_2)Fe(diphosphine)_2X]^{n+}$ complexes, which are favored by the use of diphosphine ligands that form four- or five-membered rings upon coordination to the metal.[32−35] To overcome the preference of the PNP ligand to form cis complexes, diphosphine ligands with small chelate bite angles were combined with PNP. This approach was suggested by previous structural studies of $[Ni(PNP)_2]^{2+}$ and the mixed-ligand species $[Ni(PNP)(dmpm)]^{2+}$.[23] The former has a large tetrahedral distortion, whereas the latter cation is planar. It therefore seemed reasonable that this mixed-ligand approach could be used to prepare *trans*-$[Fe(PNP)(dmpm)(X)(Y)]^{n+}$ complexes, which require a planar arrangement of diphosphine ligands. As the results described above for $[Fe(PNP)(dmpm)(CH_3CN)_2]^{2+}$, $[Fe(PNP)(dmpm)(CO)(Cl)]^+$, $[HFe(PNP)(dmpm)(Cl)]$, $[HFe(PNP)(dmpm)(CO)]^+$, and $[(H_2)Fe(PNP)(dmpm)(H)]^+$ indicate, complexes with trans geometries that incorporate the PNP ligand can be prepared using this strategy. The geometry of one of these complexes, *trans*-$[HFe(PNP)(dmpm)(CH_3CN)](BF_4)$, has been confirmed by X-ray diffraction.

Of major interest is the role of the pendant base of the PNP ligand in the chemistry of these complexes. To establish a baseline for the proton acceptor ability of this ligand on coordination to iron, the pK_a values of the protonated $PNHP^+$ ligand for *trans*-$[Fe(PNHP)(dmpm)(CH_3CN)_2]^{3+}$ (9.4), *trans*-$[Fe(PNHP)(dmpm)(Cl)(CO)]^{2+}$ (9.6), and *trans*-$[HFe(PNHP)(dmpm)(CO)]^{2+}$ (10.5) were determined in acetonitrile. To facilitate comparison on an aqueous scale, it has been suggested that aqueous pK_a values can be estimated by subtracting 7.5 from pK_a values determined in acetonitrile.[47] The observation that protonation of *trans*-$[HFe(PNP)(dmpm)(CO)]^+$ occurs at the N atom of the PNP ligand (see structure **12**), and not at the hydride ligand to form

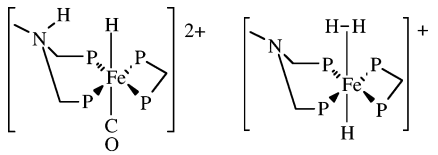

12 **13**

a dihydrogen complex, indicates that the incipient dihydrogen ligand in this complex would be more acidic than the protonated $PNHP^+$ ligand. Therefore, this

(45) Lenero, K. A.; Kranenburg, M.; Guari, Y.; Kamer, P. C. J.; van Leeuwen, P. W. N. M.; Sabo-Etienne, S.; Chaudret, B. *Inorg. Chem.* **2003**, *42*, 2859−2866.
(46) Karsch, H. H. *Chem. Ber.* **1984**, *117*, 3123−3133.
(47) Kristjánsdóttir, S. S.; Norton, J. R. In *Transition Metal Hydrides*; Dedieu, A., Ed.; VCH: New York, 1991; pp 309−359.

dihydrogen complex has a pK_a value of less than 10.5 in acetonitrile. In contrast, when a hydride ligand is trans to the dihydrogen ligand in [*trans*-[(H_2)Fe(PNP)(dmpm)(H)]$^+$ (see structure **13**), the dihydrogen ligand is less acidic than the protonated PNHP$^+$ ligand. As a result, the dihydrogen complex with a trans hydride is stable with respect to intramolecular heterolytic cleavage. The formation of [*trans*-[(H_2)Fe(PNP)(dmpm)(H)]$^+$ and *trans*-[HFe(PNHP)(dmpm)(CO)]$^{2+}$ illustrates the control of intramolecular heterolytic cleavage of the dihydrogen ligand by varying the nature of the trans ligand. It is possible that a similar effect may be achieved in the Fe-only hydrogenases by the variation of the CO ligand trans to the H_2 activation site from a bridging to a terminal position during the catalytic cycle.[15]

For *trans*-[HFe(PNP)(dmpm)(CH_3CN)]$^+$, protonation in acetonitrile leads to loss of H_2 and the formation of *trans*-[Fe(PNP)(dmpm)(CH_3CN)$_2$]$^{2+}$. This reaction presumably involves the sequence of steps shown in reaction 5. The dihydrogen intermediate *trans*-[(H_2)Fe(PNP)(dmpm)(CH_3CN)]$^{2+}$ (**16**) results from proton transfer from the PNHP$^+$ ligand of **15**, as shown in step 2. This complex is unstable with respect to loss of H_2 and coordination of acetonitrile (step 3). For the catalytic production of hydrogen, it is desirable that the elimination of hydrogen be somewhat favorable to avoid product inhibition. On the other hand, a large driving force will lead to increased overpotentials for H_2 production.

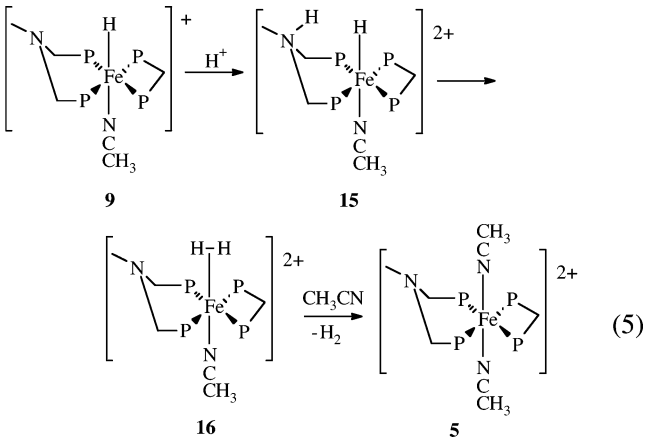

As reported previously, [Ni(PNP)$_2$]$^{2+}$ adds hydrogen to form [HNi(PNHP)(PNP)]$^{2+}$, with Ni acting as a hydride acceptor and the N atom of one diphosphine ligand acting as a proton acceptor. In contrast, *trans*-[HFe(PNHP)(dmpm)(CH_3CN)]$^{2+}$ eliminates hydrogen. Because the pK_a values for the protonated PNP ligands are the same within experimental error for these two compounds, this difference in behavior can be attributed to the greater hydride donor ability of *trans*-[HFe(PNP)(dmpm)(CH_3CN)]$^+$ (less than 61 kcal/mol) compared to [HNi(PNP)$_2$]$^+$ (67 kcal/mol).

Although the development of a more complete series of cis complexes is still in progress, our preliminary comparisons of the cis and trans Fe(II) octahedral complexes have already revealed significant reactivity differences. The observation of a half-life of less than 1 min for the loss of acetonitrile from *cis*-[Fe(PNP)$_2$(CH_3CN)$_2$]$^{2+}$ in acetonitrile-d_3, compared to a half-life of 7.2 h for [Fe(PNP)(dmpm)(CH_3CN)$_2$]$^{2+}$, indicates a rate difference of 10^2−10^3 for these cis and trans complexes. The faster rate of exchange of acetonitrile for *cis*-[Fe(PNP)$_2$(CH_3CN)(CO)]$^{2+}$ ($t_{1/2}$ = 34 min) compared to *trans*-[HFe(PNP)(dmpm)(CH_3CN)]$^+$ ($t_{1/2}$ = 9.6 h) is consistent with the longer Fe−N bond in the former complex compared to the latter. The observation of steric interactions between ethyl substituents on one PNP ligand and coordinated acetonitrile for *cis*-[Fe(PNP)$_2$(CH_3CN)(CO)]$^{2+}$ suggests steric interactions as well as electronic features could be useful in tuning the rate of ligand loss in the cis complexes. The observation that acetonitrile substitution for [Fe(PNP)$_2$(CH_3CN)$_2$]$^{2+}$ is faster than for *cis*-[Fe(PNP)$_2$(CH_3CN)(CO)]$^{2+}$ is consistent with acetonitrile being a better π donor (or at least a poorer π acceptor) than CO. For (H_2)OsHCl(CO)(P^{i}Pr$_3$)$_2$, the rate of H_2 loss is reported to be nearly 10^6 times faster than for (H_2)OsH$_2$(CO)(P^{i}Pr$_3$)$_2$.[39] In the former, the chloride ligand is cis to the dihydrogen ligand and can stabilize the five-coordinate intermediate formed by hydrogen loss through back-bonding, whereas in the latter complex, the cis hydride ligand is unable to provide a stabilizing back-bonding contribution. A more complete understanding of the kinetics of ligand exchange for the iron complexes described in this work, as well as the thermodynamic characteristics of the Fe−H, Fe−(H_2) and N−H bonds in these complexes, will be important for further efforts to develop iron-based catalysts for H_2 production/oxidation.

Summary

A number of Fe(II) complexes have been prepared containing the PNP ligand, which has a pendant nitrogen base similar to that thought to be present in Fe-only hydrogenases. The stereochemistry of these complexes can be controlled by the proper choice of a second diphosphine ligand. When this ligand is PNP, cis complexes are formed. If the second ligand is dmpm, a trans geometry results. This combination of cis and trans complexes provides an opportunity to systematically probe the role of cis and trans ligands in conjunction with a pendant base in H_2 cleavage and proton-transfer reactions. The acidity of the protonated PNP ligand has been measured for three complexes with pK_a values ranging from 9.4 to 10.5 in acetonitrile. The observation of *trans*-[HFe(PNHP)(dmpm)(CO)]$^{2+}$ indicates that intramolecular heterolytic cleavage of hydrogen is favored when CO occupies the trans position. Conversely, the observation of *trans*-[(H_2)Fe(PNHP)(dmpm)(H)]$^+$ indicates that a trans hydride ligand disfavors intramolecular heterolytic cleavage of H_2 in this series of complexes. The exchange of free and coordinated acetonitrile ligands is faster for the cis complexes compared to trans complexes and suggests possible approaches to controlling solvent and H_2 exchange.

Experimental Section

Spectral and Electrochemical Measurements. ^{1}H NMR, ^{31}P NMR, and variable-temperature NMR (VT NMR) spectra were recorded on a Varian Inova 400 MHz spectrometer. ^{1}H chemical shifts are reported relative to residual solvent protons. ^{31}P NMR spectra were proton-decoupled unless stated otherwise, and all chemical shifts are referenced to external phosphoric acid. VT NMR experiments were allowed to equili-

brate for 5 min at each temperature before spectra were recorded. T_1 measurements were made using the inversion−recovery method. Spectral simulations were performed using Nuts Software by Acron NMR Inc. Electrospray ionization (ESI) mass spectra were collected using an HP 59987A Electrospray with an HP 5989B mass spectrometer. Infrared spectra of potassium bromide pellets and solution infrared spectra were recorded on either a ThermoNicolet Avatar 360 FT-IR ESP spectrometer or a Mattson Satellite FTIR spectrometer. UV−vis spectra were recorded on an Agilent 8453 UV−vis spectrometer. Elemental analyses were performed by Desert Analytics Laboratory, Tucson, AZ.

General Methods and Materials. All reactions were performed using standard Schlenk techniques under argon or handled in a glovebox under nitrogen, and all solvents were degassed with argon. Acetonitrile, dichloromethane, ethanol, hexanes, and aniline were dried over calcium hydride and distilled prior to use. Ether, toluene, and tetrahydrofuran (THF) were dried over sodium/benzophenone and distilled. Acetone, acetone-d_6, acetonitrile-d_3, and toluene-d_8 were dried over 4 Å molecular sieves and degassed using three freeze−pump−thaw cycles. Bis(triphenylphosphine)nitrogen(1+) borohydride, bis(dimethylphosphino)methane, iron dichloride, *p*-bromoaniline, 4-cyanoaniline, anisidine, 1,1,3,3-tetramethylguanidine, fluoroboric acid (48% aqueous solution), carbon monoxide, and hydrogen were obtained from commercial suppliers and used without further purification. Deuterium (gas, 99.8%) and deuterium hydride (gas, 98%) were acquired from Isotec. $[Fe(CH_3CN)_6](BF_4)_2$ and bis((diethylphosphino)-methyl)methylamine (PNP) were prepared according to literature methods.[23,48,49]

$[Fe(PNP)_2(CH_3CN)_2](BF_4)_2$ (3). A solution of $[Fe(CH_3CN)_6](BF_4)_2$ (0.41 g, 0.86 mmol) in acetonitrile was added to a solution of bis((diethylphosphino)methyl)methylamine (PNP, 0.40 g, 1.70 mmol) in acetonitrile (total 30 mL). The red-orange solution was stirred at room temperature for 2 h. The volume of the solution was reduced to approximately 10 mL by applying a vacuum. Red crystals (0.36 g, 55%) were obtained by addition of ether to this solution and cooling to −15 °C. Anal. Calcd for $C_{26}H_{60}N_4P_4B_2F_8Fe$: C, 39.93; H, 7.73; N, 7.16. Found: C, 39.72; H, 7.64; N, 7.15. ^{31}P NMR (CD_3CN; ppm): δ_A 22.01, δ_B 14.50, $^2J_{AA'} = -26.7$ Hz, $^2J_{BB'} = 49.6$ Hz, $^2J_{AB} = 43.2$ Hz, $^2J_{AB'} = 67.2$ (see structure **3** of the text for atom labeling scheme). ^{1}H NMR (CD_3CN; ppm): 2.36 (m), 2.81 (m), 3.16 (m), 3.34 (m) (2 H each, PCH_2N); 2.45 (s, 5.7 H, NCH_3); 1.48 (m), 1.64 (m), 1.79 (m), 1.99 (m), 2.12 (m), 2.24 (m) (16 H total, PCH_2CH$_3$); 1.07 (m), 1.15 (m), 1.23 (m) (24 H total, PCH$_2$$CH_3$); 1.96 (s, 6.8 H, C$H_3$CN). ESI$^+$ (CH_3CN; *m/z*): 695 $\{[Fe(PNP)_2(CH_3CN)_2](BF_4)\}^+$, 613 $\{[Fe(PNP)_2](BF_4)\}^+$, 545 $\{[Fe(PNP)_2](F)\}^+$. IR (KBr pellet; cm^{-1}): ν_{CN} 2324 and 2290.

$[Fe(PNP)_2(CO)(CH_3CN)](BF_4)_2$ (4). Carbon monoxide was bubbled into a solution of $[Fe(PNP)_2(CH_3CN)_2](BF_4)_2$ (0.10 g, 0.13 mmol) in acetone (40 mL) for 20 min. The reaction flask was closed, and then the solution was stirred overnight. The volume of the solution was reduced to ca. 15 mL by applying a vacuum, and then ether was added with stirring until the solution began to get cloudy. Crystals formed upon cooling to −15 °C for 2 weeks (0.035 g, 36%). Anal. Calcd for $C_{25}H_{57}ON_3P_4B_2F_8Fe$: C, 39.04; H, 7.47; N, 5.46. Found: C, 39.10; H, 7.26; N, 5.26. ^{31}P NMR (acetone-d_6; ppm): δ_Z 2.12 (ddd), δ_X 11.62 (ddd), δ_M 16.68 (ddd), and δ_A 18.93 (ddd). $^2J_{ZX} = 46.2$ Hz, $^2J_{MZ} = 69.2$ Hz, $^2J_{MX} = 54.0$, $^2J_{AZ} = 48.9$ Hz, $^2J_{AX} = 62.2$ Hz, $^2J_{AM} = -38.4$ Hz (see structure **4** in text for atom-labeling scheme). ^{1}H NMR (acetone-d_6; ppm): 3.16 (m), 3.40 (m), 3.60 (m), 3.78 (m), 4.15 (s) (8 H total, PCH_2N); 2.70 (s, 3 H, CH_3-CN); 2.61 (s), 2.54 (s) (3 H each, NCH_3); 2.47 (m), 2.26 (m), 2.01 (m) (16 H total, PCH_2CH$_3$); 1.10−1.50 (br m, 24 H, PCH$_2$$CH_3$). IR (KBr; cm^{-1}): ν_{CO} 2032 and 1981. IR (CD_2Cl_2; cm^{-1}): ν_{CO} 1991 cm^{-1}.

Attempted Preparation of $[Fe(PNP)(dppm)(CH_3CN)_2](BF_4)_2$. PNP (20.2 μL, 0.070 mmol) was added, by syringe, to a solution of $[Fe(CH_3CN)_6](BF_4)_2$ (33.3 mg, 0.070 mmol) in acetonitrile-d_3 (0.7 mL). After 30 min, this solution was added to dppm (0.0268 g, 0.070 mmol), and the resulting solution was monitored by ^{31}P NMR for 6 days. A mixture of products was observed at all times. The major components were assigned to *trans*-$[Fe(PNP)(dppm)(CH_3CN)_2](BF_4)_2$ (an AA′XX′ spin pattern at 5.51 ppm (dppm) and 25.32 ppm (PNP)) and *cis*-$[Fe(PNP)_2(CH_3CN)_2](BF_4)_2$ (two second-order multiplets at 22.02 and 14.52 ppm as discussed above). Three other unidentified singlets were observed at 12.5, 39.6, and 32.4 ppm.

$[Fe(PNP)(dmpm)(CH_3CN)_2](BF_4)$ (5). A solution of $[Fe(CH_3CN)_6](BF_4)_2$ (0.697 g, 1.46 mmol) in acetonitrile was added to a solution of PNP (0.344 g, 1.46 mmol) and dmpm (0.232 mL, 1.46 mmol) in acetonitrile (total 50 mL), and the resulting red-orange solution was stirred at room temperature for 1 h. Removal of the solvent with a vacuum resulted in a tar. Red-orange crystals were obtained by crystallization from a solvent mixture of dichloromethane and ethanol (0.55 g, 55%). Anal. Calcd for $C_{20}H_{47}N_3P_4B_2F_8Fe$: C, 35.17; H, 6.93; N, 6.15. Found: C, 34.89; H, 6.98; N, 5.88. ^{1}H NMR (CD_3CN; ppm): 2.40 (s, 5.5 H, CH_3CN); 3.59 (t, 2.4 H, PCH_2P, $^2J_{PH} = 11.2$ Hz); 1.62 (t, 11.5 H, $^2J_{PH} = 10.0$ Hz, PCH_3); 2.87 (s, 3.8 H, PCH_2N); 2.50 (s, 2.9 H, NCH_3); 1.80 (m, 8.1 H, PCH_2CH$_3$); 1.11 (m, 12.0 H, PCH$_2$CH_3). ^{31}P NMR (CD_3CN; ppm): δ_A −5.06 (dmpm); δ_X 29.15 (PNP); $^2J_{AA'} = 78.6$ Hz, $^2J_{AX} = 89.3$ Hz, $^2J_{AX'} = -57.2$, $^2J_{XX'} = 55.5$ Hz. ESI$^+$ (CH_3CN; *m/z*): 514 $\{[Fe(PNP)(dmpm)(CH_3CN)_2](BF_4)\}^+$; 446 $\{[Fe(PNP)(dmpm)(CH_3CN)_2](F)\}^+$. IR (KBr; cm^{-1}): ν_{CN} 2261, $\nu_{BF_4} = 1051$.

$[Fe(Cl)_2(PNP)(dmpm)]$ (6). A mixture of PNP (0.240 g, 1.02 mmol) and dmpm (0.160 g, 1.17 mmol) in 5 mL of toluene was added to a suspension of $FeCl_2$ (0.129 g, 1.02 mmol) in 60 mL of toluene, and the resulting green solution was stirred for 3 h. Removal of the solvent with a vacuum resulted in an oil. Emerald green crystals (0.215 g, 43%) were obtained by crystallization from hexanes at −15 °C. Anal. Calcd for $C_{16}H_{41}NP_4Cl_2Fe$: C, 38.58; H, 8.30; N, 2.81. Found: C, 38.89; H, 8.32; N, 2.88. NMR spectra were not observed due to the paramagnetic nature of this compound. ESI+ (CH_3CN; *m/z*): 462 [FeCl(PNP)(dmpm)]$^+$. UV−vis (THF): λ_{max} 411 nm, λ_{max} 673 nm, $\epsilon = 17$ M^{-1} cm^{-1}.

$[Fe(Cl)(CO)(PNP)(dmpm)]_2(FeCl_4)$ (7). A mixture of PNP (0.624 g, 2.65 mmol) and dmpm (0.362 g, 2.66 mmol) in toluene (10 mL) was added to a suspension of $FeCl_2$ (0.337 g, 2.66 mmol) in toluene (100 mL), and the resulting emerald green solution was stirred for 3 h. Carbon monoxide was bubbled into this solution for 40 min. A yellow precipitate formed when this solution was stirred overnight under a CO atmosphere. Removal of the solvent with a vacuum resulted in a yellow powder. Yellow-orange crystals (0.209 g, 20%) were obtained by crystallization from warm acetone under CO. Anal. Calcd for $C_{34}H_{82}N_2P_8Cl_6O_2Fe_3$: C, 34.64; H, 7.01; N, 2.38. Found: C, 34.55; H, 7.35; N, 2.36. ^{1}H NMR (CD_3CN; ppm): 2.74 (m, 2.1 H, PCH_2P); 0.88 (m), 0.94 (m) (15.2 H total, PCH_3); 2.49 (m, 2.1 H, PCH_2N); 2.29 (s, 3.1 H, NCH_3); 1.63 (br m, 6.6 H, PCH_2-CH_3); 0.03 ppm, 0.29 (br s, 12.0 H, PCH$_2$CH_3). ^{31}P NMR (CD_2Cl_2; ppm): AA′XX′ spin pattern; δ_A −9.64 (dmpm), δ_X 29.46 (PNP); $^2J_{AA'} = 91.0$ Hz, $^2J_{AX} = 123.1$ Hz, $^2J_{AX'} = -60.6$, $^2J_{XX'} = 59.2$ Hz. ESI$^+$ (CH_3CN; *m/z*): 490 $\{[Fe(Cl)(CO)(PNP)(dmpm)]\}^+$. IR (KBr; cm^{-1}): ν_{CO} 1918 and 1923. IR (CH_2Cl_2; cm^{-1}): ν_{CO} 1936.

$[HFe(Cl)(PNP)(dmpm)]$ (8). A solution of $[FeCl_2(PNP)(dmpm)]$ (0.700 g, 1.40 mmol) in tetrahydrofuran (50 mL) was added to a suspension of $PPNBH_4$ (1.55 g, 2.80 mmol) in tetrahydrofuran (100 mL). The resulting orange solution was stirred for 2 h. The white precipitate was removed by filtration, and the solvent was removed from the filtrate with a vacuum

(48) Hathaway, B. J.; Underhill, A. E. *J. Chem. Soc.* **1960**, 3705−3711.
(49) Heintz, P. A.; Smith, J. A.; Szalay, P. S.; Weisgerber, K. R. *Inorg. Synth.* **2002**, *33*, 77.

to yield a red-orange solid. Orange feathery crystals were obtained by dissolving this solid in hexanes and cooling at −15 °C overnight (0.205 g, 32%). The product was isolated by filtration. Anal. Calcd for $C_{16}H_{42}NP_4ClFe$: C, 41.44; H, 9.12; N, 3.02; Cl, 7.64. Found: C, 41.33; H, 9.03; N, 3.06; Cl, 7.57. ^{31}P NMR (toluene-d_8; ppm): δ_A 3.96 (dmpm), δ_X 48.26 (PNP). ^{1}H NMR (acetone-d_6; ppm): −27.00 (pentet, $^2J_{PH}$ = 47 Hz, 1 H, *H*Fe); 1.06 (br m, 12 H, PCH_2CH_3); 1.50 (br m, 14.3 H, PCH_3); 1.67 (m), 1.79 (m), 1.89 (m) (7.1 H total, PCH_2CH_3); 2.33 (s, 3.0 H, NCH_3); 2.69 (m), 2.68 (m) (2 H each, PCH_2N); 3.02 (m), 3.30 (m) (1 H each, PCH_2P). ESI$^+$ (CH_3CN; *m/z*): 428 {[HFe(PNP)(dmpm)]}$^+$, 462 {[Fe(Cl)(PNP)(dmpm)]}$^+$, 469 {[HFe(CH_3CN)(PNP)(dmpm)]}$^+$. IR (KBr; cm^{-1}): ν_{FeH} 1793.

[HFe(CH_3CN)(PNP)(dmpm)][BPh_4] (9). [HFeCl(PNP)(dmpm)] (0.207 g, 0.446 mmol) and $NaBPh_4$ (1.408 g, 4.11 mmol) were added to a flask containing acetonitrile (150 mL). The resulting yellow solution was stirred for 2 h, and the product was precipitated by addition of water to form a solid that was washed with ether. Yellow crystals (0.077 g, 23%) were obtained from acetonitrile/ether solutions at −15 °C. Anal. Calcd for $C_{42}H_{65}N_2P_4BFe$: C, 63.97; H, 8.31; N, 3.55. Found: C, 63.22; H, 8.05; N, 3.33. ^{31}P NMR (CD_3CN; ppm): AA′XX′ spin pattern; δ_A 3.32 (dmpm), δ_X 44.86 (PNP). ^{1}H NMR (CD_3CN; ppm): −19.85 (ttd, $^2J_{PH}$ = 49 Hz, $^2J_{PH}$ = 43 Hz, $^4J_{HH}$ = 4 Hz, 1 H, *H*Fe); 1.05 (br m, 12.5 H, PCH_2CH_3); 1.45 (t), 1.53 (t) ($^2J_{PH}$ = 4 Hz, 12.3 H total, PCH_3); 1.49 (m), 1.60 (m), 1.69 (m) (8.3 H total, PCH_2CH_3); 2.33 (s, 3.0 H, NCH_3); 2.35 (m), 2.81 (m) (2 H each, PCH_2N); 2.99 (m), 3.14 (m) (1 H each, PCH_2P); 2.22 (s, 3.0 H, $NCCH_3$); 6.85 (m), 6.99 (m), 7.27 (m) (20.1 H total, $B(C_6H_5)_4$). Broadband ^{31}P-decoupled ^{1}H NMR (CD_3CN; ppm): −19.85 (d, $^2J_{HH}$ = 4 Hz, *H*Fe); 2.89 and 3.15 (AB portion of ABX spin pattern, $^2J_{HH}$ = 13 Hz, $^4J_{HH}$ = 4 Hz, PCH_2P). Broadband ^{31}P-decoupled ^{1}H gCOSY (CD_3CN; ppm; see Figure S2): −19.85 (*H*Fe) correlated to 3.15 (one H of PCH_2P). Selective ^{31}P-decoupled (PNP) ^{1}H NMR (CD_3CN; ppm): −19.85 (br t, $^2J_{PH}$ = 49 Hz, *H*Fe). Selective ^{31}P-decoupled (dmpm) ^{1}H NMR (CD_3CN; ppm): −19.85 (br t, $^2J_{PH}$ = 43 Hz, *H*Fe). ESI$^+$ (CH_3CN; *m/z*): 428 {[HFe(PNP)(dmpm)]}$^+$. IR (KBr; cm^{-1}): ν_{FeH} 1826; ν_{CN} = 2230.

[HFe(CO)(PNP)(dmpm)][PF_6]/[Fe(Cl)(CO)(PNP)(dmpm)][PF_6], (10-PF_6/7-PF_6) Mixture. Acetone (60 mL) was added to a mixture of [HFeCl(PNP)(dmpm)] (0.110 g, 0.237 mmol) and $NaPF_6$ (0.130 g, 0.774 mmol) in a Schlenk flask. The resulting solution was purged with CO for 20 min and then stirred under a CO atmosphere overnight. The solvent was removed under vacuum to give a yellow oil that was extracted with CH_2Cl_2 (2 × 20 mL). Ether was added to the combined extracts. Yellow crystals (0.050 g) formed upon cooling overnight to −15 °C. The following data indicated a mixture of products. Similar mixtures were also obtained in NMR tube experiments. ^{31}P NMR (acetone-d_6; ppm): −143.15 (septet, PF_6), −7.74 (AA′XX′ spin pattern, 17%, [Fe(Cl)(CO)(PNP)(*dmpm*)](PF_6)); 28.91 (AA′XX′ spin pattern, 18%, [Fe(Cl)(CO)(*PNP*)(dmpm)](PF_6)); 2.34 (AA′XX′ spin pattern, 30%, [HFe(CO)(PNP)(*dmpm*)](PF_6)); 44.29 (AA′XX′ spin pattern, 30%, [HFe(CO)(*PNP*)(dmpm)](PF_6)). ^{31}P gCOSY (acetone-d_6; ppm): −7.74 ([Fe(Cl)(CO)(PNP)(*dmpm*)](PF_6)) correlated to 28.91 ([Fe(Cl)(CO)(*PNP*)(dmpm)](PF_6)); 2.34 ([HFe(CO)(PNP)(*dmpm*)](PF_6)) correlated to 44.29 ([HFe(CO)(*PNP*)(dmpm)](PF_6)). ^{1}H NMR (acetone-d_6; ppm): −7.06 (ttd, $^2J_{PH}$ = 52 Hz, $^2J_{PH}$ = 42 Hz, $^4J_{HH}$ = 3.5 Hz, 1.3 H, *H*Fe (**10**)); 1.09−1.31 (m, 24 H, PCH_2CH_3 (**7** and **10**)); 1.75 (m), 1.81 (m) (19.6 H total, PCH_3 (**7** and **10**)); 1.52 (m), 1.89 (m), 1.97 (m), 2.10 (m) (16.2 H, PCH_2CH_3 (**7** and **10**)); 2.39 (s), 2.48 (s) (3.56 and 2.28 H, respectively, NCH_3 (**7** and **10**)); 2.32 (m), 3.06 (m) (PCH_2N (**7** and **10**)); 3.40 (m, PCH_2P (**7** and **10**)). Broadband ^{31}P-decoupled ^{1}H NMR (acetone-d_6; ppm): −7.05 (d, $^4J_{HH}$ = 3.5 Hz, *H*Fe (**10**)); 3.40 and 3.46 (AB portion of ABX spin pattern, $^2J_{HH}$ = 15 Hz, $^4J_{HH}$ = 3.5 Hz, PCH_2P (**10**)). Broadband ^{31}P-decoupled ^{1}H gCOSY (acetone-d_6): −7.05 (*H*Fe) correlated to 3.41 (one H of PCH_2P).

Observation of [HFe(H_2)(PNP)(dmpm)]Cl. In a typical experiment, acetone-d_6 (0.7 mL) was cooled to 0 °C, degassed with H_2, and syringed into an NMR tube containing [HFe(Cl)(PNP)(dmpm)] (20 mg, 40 μmol), tetramethylguanidinium triflate ([HTMG][OTf], 11.4 mg, 43 μmol), and H_2 (1 atm). The sample was kept at 0 °C for 1.5 h before the VT NMR experiments were performed. ^{31}P NMR (acetone-d_6, −60 °C; ppm): −6.65 (m, [HFe(H_2)(PNP)(*dmpm*)]); 31.29 (m, [HFe(H_2)(*PNP*)(dmpm)]); 4.3 (br, [HFe(Cl)(PNP)(*dmpm*)]); 48.7 (br, [HFe(Cl)(*PNP*)(dmpm)]); 50.64 (d, impurity); 6.73 (br m, impurity). ^{1}H NMR (acetone-d_6, −60 °C; ppm): −11.76 (pentet, 1.0 H, $^2J_{PH}$ = 46 Hz, [*H*Fe(H_2)(PNP)(dmpm)]$^+$); −7.90 (br s, 2.0 H, [HFe(*H_2*)(PNP)(dmpm)]$^+$). T_1 data for [*H*Fe(H_2)(PNP)(dmpm)]$^+$ (400 MHz): 0.346 s at 183 K, 0.317 s at 193 K, 0.0957 s at 213 K, 0.0707 s at 233 K, 0.0872 s at 253 K. T_1 data for [HFe(*H_2*)(PNP)(dmpm)]$^+$: 0.0207 s at 183 K, 0.0229 s at 193 K, 0.0377 s at 213 K, 0.0639 s at 233 K, 0.0841 s at 253 K, 0.0986 s at 273 K. A plot of ln T_1 versus 1/*K* is shown in Figure S3 in the Supporting Information. Using T_1^{min} = 0.0207 s and the equations $d_{HH}(fast) = 4.61[T_1^{min}/\nu]^{1/6}$ and $d_{HH}(slow) = 5.81[T_1^{min}/\nu]^{1/6}$ gives d_{HH} values of 0.89 and 1.12 Å for fast and slow rotation, respectively.[36−38] In these equations, *d* is in Å, T_1^{min} is in s, and the spectrometer frequency, ν, is in MHz.

$^1J_{HD}$ Experiments. Acetone saturated with HD was syringed into an NMR tube containing [HFe(Cl)(PNP)(dmpm)] (20 mg, 40 μmol), (DTMG)(OTf) (11.4 mg, 43 μmol), and HD gas (1 atm). An additional quantity of HD gas (approximately 3 mL) was added with a syringe. The sample was maintained at 0 °C for 1.5 h before the VT NMR experiments were run. ^{2}H NMR (acetone, −60 °C): −8.01 (d, $^1J_{HD}$ = 30.8 Hz, [(HFe(H*D*)(PNP)(dmpm)]$^+$). This doublet collapsed to a singlet when the spectrum was proton decoupled (all the other peaks remained the same). Using this $^1J_{HD}$ value and $d_{HH} = 1.42 - 0.0167(J_{HD})$, a value of 0.90 Å is calculated for the HH bond distance.[41] Using $d_{HH} = 1.44 - 0.0168J_{HD}$, a value of 0.92 Å is calculated for the HH bond distance.[40]

pK_a Measurements. In a typical experiment, [Fe(Cl)(CO)(PNP)(dmpm)]$^+$ (25 mg, 0.021 mmol), *p*-bromoanilinium tetrafluoroborate (55 mg, 0.21 mmol), and *p*-bromoaniline (36 mg, 0.21 mmol) were weighed into an NMR tube and dissolved in CD_3CN (0.7 mL). The solution was monitored by ^{31}P NMR for several hours at 23 ± 2 °C to ensure that the ^{31}P NMR shifts were constant; however, equilibrium occurred in less than 0.5 h. This experiment was repeated using 5-, 10-, and 15-fold excesses of 1:1 mixtures of *p*-bromoanilinium tetrafluoroborate/*p*-bromoaniline (BH^+/B) based on the metal complex. The ratio of [Fe(CO)(Cl)(PNHP)(dmpm)]$^{2+}$/[Fe(CO)(Cl)(PNP)(dmpm)]$^+$, $(1 - x)/x$, was calculated using the observed ^{31}P NMR shift of the PNP ligand, δ(PNP), and the relationship $x(29.08\text{ ppm}) + (1 - x)(37.39\text{ ppm}) = \delta(\text{PNP})$. In this equation, *x* is the mole fraction of [Fe(CO)Cl)(PNP)(dmpm)]$^+$ and $1 - x$ is the mole fraction of [Fe(CO)(Cl)(PNHP)(dmpm)]$^{2+}$. With no acid added, the ^{31}P NMR chemical shift observed for the PNP ligand of [Fe(CO)(Cl)(PNP)(dmpm)]$^+$ is 29.08 ppm. The shift of the completely protonated PNP ligand, observed when 3 equiv of HBF_4 was added to form [Fe(CO)(Cl)(PNHP)(dmpm)]$^{2+}$, is 37.39 ppm. The ratio of [B]/[BH^+] was held constant at 1.0 using large excesses of both B and BH^+. The equilibrium constant ($K_{eq}(4)$ = {[B]/[BH^+]} × {[Fe(CO)(Cl)(PNHP)(dmpm)]$^{2+}$}/{[Fe(CO)(Cl)(PNP)(dmpm)]$^+$}) calculated for three experiments was 1.1 ± 0.2 (where the uncertainty represents two standard deviations). Addition of log $K_{eq}(4)$ to the pK_a value of *p*-bromoanilinium (9.6) in acetonitrile[40] gives a pK_a value of 9.6 ± 0.2 for [Fe(CO)(Cl)(PNHP)(dmpm)]$^{2+}$. The uncertainty in the pK_a value reflects uncertainties in both the measurement (±0.1 at 2σ) and the reference base (±0.1).

A similar procedure was used to determine the pK_a values shown below reaction 4 for [Fe(PNHP)(dmpm)(CH_3CN)$_2$]$^{3+}$ and [HFe(PNHP)(dmpm)(CO)]$^{2+}$ cations. In the latter case, a

mixture of $[HFe(PNP)(dmpm)(CO)]^+$ and $[Fe(Cl)(CO)(PNP)(dmpm)]^+$ was used. This mixture was prepared as described above.

Determination of $t_{1/2}$ for Acetonitrile Loss. $[Fe(PNP)_2(CH_3CN)(CO)](BPh_4)_2$ (approximately 20 mg) was dissolved in 0.7 mL of acetonitrile-d_3 at 23 ± 2 °C, and the normalized integral of the acetonitrile resonance at 2.37 ppm in the proton NMR was followed as a function of time. A first-order plot of these data is shown in Figure S1(a) in the Supporting Information. The half-life obtained in this manner was 20 min. A similar procedure was used to determine half-lives of less than 1 min for $[Fe(PNP)_2(CH_3CN)_2](BF_4)_2$, 7.2 h for $[Fe(PNP)(dmpm)(CH_3CN)_2](BF_4)_2$, and 9.6 h for $[HFe(PNP)(dmpm)(CH_3CN)](BPh_4)$ (Figure S1(b) in the Supporting Information). Similar experiments were also performed for $[Fe(PNP)_2(CH_3CN)(CO)](BPh_4)_2$ ($t_{1/2} = 34$ min) and $[Fe(PNP)_2(CH_3CN)_2](BF_4)_2$ ($t_{1/2} \approx 1$ min) using acetone-d_6 as the solvent by addition of a 10-fold excess of CD_3CN.

X-ray Diffraction Studies of $[HFe(CH_3CN)(PNP)(dmpm)]BPh_4$. Crystals suitable for X-ray diffraction studies were grown from an acetonitrile/ether mixture. A crystal of dimensions 0.97 × 0.49 × 0.25 mm was mounted on a glass fiber using Paratone-N oil, transferred to a Siemens SMART diffractometer/CCD area detector, centered in the beam (Mo Kα; $\lambda = 0.71073$ Å; graphite monochromator), and cooled to −127 °C by a nitrogen low-temperature apparatus that had been previously calibrated by a thermocouple placed at the same position as the crystal. Preliminary orientation matrix and cell constants were determined by collection of 60 10-s frames, followed by spot integration and least-squares refinement. A minimum of a hemisphere of data was collected using 0.3° ϖ scans at 30 s per frame. The raw data were integrated and the unit cell parameters refined using Saint. Data analysis was performed using XPREP. Absorption correction was applied using SADABS. The data were corrected for Lorentz and polarization effects, but no correction for crystal decay was applied. Structure solutions and refinements were performed (SHELXTL-Plus V5.0) on F^2.

Preliminary data indicated a triclinic cell. Systematic absences indicated space group $P\bar{1}$ (No. 2). The choice of the centric space group was supported by the successful solution and refinement of the structure. All non-H atoms were refined anisotropically. H atoms were placed in idealized positions and were included in structure factor calculations but were not refined (with the exception of the hydride ligand). Crystallographic data and structure refinement data for $[(H)Fe(PNP)(dmpm)(CH_3CN)]BPh_4$ are shown in Table 2.

X-ray Diffraction Studies of $[Fe(PNP)_2(CH_3CN)(CO)](BPh_4)_2$. Anion exchange between $[Fe(PNP)_2(CO)(CH_3CN)](BF_4)_2$ and $Na(BPh_4)$ was used to produce the $[Fe(PNP)_2(CO)(CH_3CN)](BPh_4)_2$ salt. Crystals suitable for X-ray diffraction studies were grown from an acetone/ether mixture. A crystal of dimensions 0.45 × 0.5 × 0.55 mm was mounted on a glass fiber, and preliminary orientation matrix and cell constants were determined as described above. These data indicated a monoclinic cell, and the $P2_1/n$ space group was assigned. The structure was refined as described in the preceding paragraph for $[HFe(CH_3CN)(PNP)(dmpm)]BPh_4$, and the crystallographic data and structure refinement data for $[Fe(PNP)_2(CO)(CH_3CN)](BPh_4)_2$ are shown in Table 2.

Table 2. Crystal Data and Structure Refinement for $[(H)Fe(PNP)(dmpm)(CH_3CN)]BPh_4$ and $[Fe(PNP)_2(CH_3CN)(CO)](BPh_4)_2$

	$[(H)Fe(PNP)(dmpm)(CH_3CN)]BPh_4$	$[Fe(PNP)_2(CH_3CN)_2](BPh_4)_2$
formula	$C_{44}H_{68}BFeN_3P_4$	$C_{73}H_{97}B_2FeN_3OP_4$
formula wt	829.55	1233.89
cryst syst	triclinic	monoclinic
a (Å)	11.7581(5)	21.873(10)
b (Å)	12.0235(6)	13.629(6)
c (Å)	17.3035(8)	24.754(11)
α (deg)	105.7990(10)	90
β (deg)	95.9700(10)	109.824(10)
γ (deg)	98.8340(10)	90
V (Å^3)	2298.40(18)	6942(6)
space group	$P\bar{1}$ (No. 2)	$P2_1/n$ (No. 14)
Z	2	4
calcd density (g/cm^3)	1.199	1.181
λ(Mo Kα) (Å)	0.71073	0.71073
temp (K)	153	154
scan type, deg	ω scans, 0.3	ω scans, 0.3
θ range (deg)	1.79−27.48	1.73−27.48
no. of indep rflns	17 440 (R(int) = 0.0468)	15 911 (R(int) = 0.3327)
no. of rflns obsd	10 414	53 474
abs coeff (mm^{-1})	0.500	0.353
R1 (for $F_o > 4\sigma F_o$)[a]	0.0540 for 8537 data	0.1074 for 5699 data
R1, wR2 (all data)[b]	0.0658, 0.1515	0.2638, 0.3062
GOF[c]	1.016	0.896
largest peak, hole (e/Å^{-3})	0.864, −0.667	1.233, −1.421

[a] $R = R1 = \Sigma||F_o| - |F_c||/\Sigma|F_o|$. [b] $R_w = wR2 = [\Sigma[w(F_o^2 - F_c^2)^2]/\Sigma[w(F_o^2)^2]]^{1/2}$. [c] $GOF = S = [\Sigma[w(F_o^2 - F_c^2)^2]/(M - N)]^{1/2}$, where M is the number of reflections and N is the number of parameters refined.

Acknowledgment. This research was supported by the National Science Foundation (Grant No. CHE-0240106). NMR instrumentation used in this work was supported in part by the National Science Foundation CRIF program (Grant No. CHE-0131003). D.L.D. wishes to acknowledge the support of the United States Department of Energy, Office of Science, Chemical and Biological Sciences Division under Contract No. DE-AC36-99GO10337.

Supporting Information Available: Figures giving kinetic plots for ligand loss, the broadband ^{31}P-decoupled ^1H gCOSY NMR spectrum of $[HFe(PNP)(dmpm)(CH_3CN)](BPh_4)$, T_1 plots for $[(H_2)Fe(PNP)(dmpm)(H)]^+$, and a thermodynamic cycle and X-ray structural data, including tables of crystal and refinement data, atomic positional and thermal parameters, and interatomic distances and angles for $[HFe(PNP)(dmpm)CH_3CN)](BPh_4)$ and $[Fe(PNP)_2(CH_3CN)(CO)](BPh_4)_2$; X-ray data are also given as CIF files. This material is available free of charge via the Internet at http://pubs.acs.org.

OM050071C